Automatically generated model for light alkene combustion

Automatically Generated Model for Light Alkene Combustion

Gianmaria **PIO**[1], Xiaorui **DONG**[2], Ernesto **SALZANO**[1] William H. **GREEN**[2,*]

[1] *Department of Civil, Chemical, Environmental, and Materials Engineering – DICAM*
Alma Mater Studiorum - University of Bologna - Bologna, Italy (IT)
[2] *Department of Chemical Engineering, Massachusetts Institute of Technology, Cambridge, MA (USA)*
** Author to whom correspondence should be addressed: whgreen@mit.edu*

ABSTRACT
Light alkenes are common combustion intermediates for a variety of fuels. Therefore, understanding their oxidation and pyrolysis chemistry is key to building detailed mechanisms for heavier fuels. This work was focused on the development and evaluation of a detailed kinetic mechanism suitable for the combustion of light alkenes up to C_4 without the use of tuned parameters, instead, the parameter values come from first principles or direct measurements. The generated mechanism accurately estimates the laminar burning velocity (S_u) and ignition delay time (IDT) of light alkenes available in the literature, which represent fundamental combustion properties at a wide range of conditions. Because each parameter is thought to have a physically realistic value, not tuned to these measurements, the new model could be used as a sub-mechanism in models for other applications.
The reaction network was generated with the open-source Reaction Mechanism Generator (RMG) software. Sensitivity analyses were performed under wide ranges of temperatures and pressures, allowing for the identification of the most impactful species and reactions. Based on these, a comprehensive thermochemistry database, including calculations on 550 molecules performed in this work at the CBS-QB3 level of theory, and a kinetic library, including theoretically-derived reaction rates retrieved from the literature, were built and used in the mechanism generation. The developed mechanism was compared against several existing detailed kinetic mechanisms for ethene, propene, 1-butene, 2-butene, and isobutene. The newly generated model is the most accurate among the ones analyzed, in terms of fractional bias and normalized mean square error. Hence, this new model was used to analyze the chemistry of alkene combustion. Key rate coefficients were compared, to identify the cause of deviations between the models and possible areas for further improvements.

Keywords: Detailed kinetic mechanisms, Alkene combustion, Laminar burning velocity, Ignition delay time, Butenes

Highlights

1) Construction of a comprehensive library of thermochemical data
2) Development and validation of the detailed kinetic mechanism without tuned parameters
3) Comparison of new and existing kinetic models with experimental measurements
4) Identification of possible causes of low accuracy
5) Implementation of statistical analysis for the evaluation of mechanisms' accuracy

1. Introduction

The increasing availability of affordable and optimized computational tools allows the implementation of detailed kinetic mechanisms for the characterization of complex combustion [1] and chemical processes [2]. Towards building mechanisms for large and complex fuels, knowledge of the chemistry of smaller intermediate molecules under a wide range of conditions is essential. Among these smaller molecules, light alkenes (e.g., ethylene, propene, and butenes) are important in the combustion and pyrolysis of many fuels [3], including oxygenated biofuels (e.g., butanols and butyl acetates) [4]. They are usually produced by beta-scission reactions from radical species resulting from hydrogen abstraction [5] or by unimolecular reactions from larger alkenes (e.g., retro-ene) [6]. Without correct sub-mechanisms of light alkenes being included, there is no guarantee larger models can make accurate predictions for key properties like ignition delay time (IDT) or laminar burning velocity (S_u). Several detailed kinetic mechanisms for alkene combustion can be found in the current literature. Table 1 presents a list of available mechanisms, partially included in the recently published review by Jach et al. (2019) [7]. The reported list represents an inclusive collection of kinetic mechanisms including light alkene chemistry, and each mentioned mechanism has been developed by highly reputed kinetics groups and validated by experiments. However, there is a lack of agreement regarding the species and reactions included in these models, and also disagreements about the values of the rate and thermochemical parameters, resulting in large variability in the prediction of experimental observables such as IDT or S_u [8]. The lack of a consensus for these light alkene networks raises confusion in selecting an optimal 'core' for model development. Hence, there remains an urgent need in the field to develop an accepted 'standard' mechanism for light alkenes.

Table 1. Overview of the kinetic mechanisms available in the current literature.

Mechanism	Year of release	Number of species	Distinguishes butene isomers
USC Mech C1-C3 [9]	1999	71	No
GRI-mech 3.0 [10]	1999	53	No
Konnov 0.5 [11]	2000	127	No
Creck (C1C3 HT NOx) [12]	2003	115	No
CaltechMech [13]	2007	174	No
USC Mech II [14]**	2007	111	Yes
JetSurF 2.0 [15]* **	**2010**	**348**	**Yes**
NUIG (Butane) [16]**	2010	230	Yes
LLNL (n-Heptane) [17]* **	**2011**	**654**	**Yes**
LLNL (Butanol) [18]* **	**2011**	**431**	**Yes**
MIT (Butanol) [19]* **	**2011**	**263**	**Yes**
Bielefeld University (Butene) [20]**	2013	163	Yes
Creck (C1C3 LT HT) [21]	2014	107	No
UC San Diego [22]	2014	50	No
NUIG (Pentane Isomers) [23]**	2015	293	Yes
NUIG (n-Hexane) [24]**	2015	1120	Yes
CNRS-INSIS Orleans (Butene) [25]*, * **	**2015**	**201**	**Yes**
NUIG (n-Heptane) [26]**	2016	1268	Yes
AramcoMech2.0 [27]**	2013	493	Yes
Lund University (Propanal) [28]	2018	119	No
AramcoMech3.0 [29]* **	**2018**	**581**	**Yes**
Creck (C1-C16 HT+LT mechanism) [30]* **	**2019**	**488**	**Yes**
Princeton (Butane) [31]	2019	148	Yes

* Model validated for atmospheric pressure, only
** This model is a subset of a later model
*** Highlighted mechanisms are used for the model comparison

The construction of these large mechanisms (hundreds or thousands of reactions) is facilitated by automated generation strategies. These strategies can be distinguished based on the approaches adopted for the selection of species/reactions and the generation of parameters. Commonly, reaction families are defined to find possible reactions and thereby extend the network from a starting pool of molecules. Packages like Genesys [32] have implemented a rule-based method, i.e., the inclusion of species and reactions in the mechanism is determined by the agreement with a set of user-defined constraints. This approach is computationally cheap, but the subjectivity of the constraints can bias model generation and does not guarantee the comprehensiveness of the generated model. Alternatively, the Reaction Mechanism Generator (RMG) [33] software has implemented a rate-based method, where the significance of a species or a reaction is determined based on simulation data. This method is more objective but more computationally costly. It can provide a more comprehensive mechanism than other methodologies if RMG includes all the important reaction families and its parameter estimates are accurate. In this light, models resulting from the first approach (e.g., [15,17,18,25]) can be considered as a reference for the evaluation of the models deriving from the latter methodology (e.g., [12,19]).

Regardless of the adopted approach, the quality of the thermochemical and kinetic parameters is essential. There are several sources for generating parameters, including experimental measurements, quantum mechanics calculations, and estimations based on the fuel structure [34]. Experimental measurements and quantum mechanics calculations are usually expensive and time-demanding. On the other hand, estimations like those from group additivity (GA) [35] and rate rules, are much computationally cheaper, but less accurate and usually only accurate for certain classes of molecules and reactions. Given the large number of species and reactions in a detailed mechanism, it is impractical to determine all of its parameters using trustworthy experiments or high-accuracy quantum chemistry calculations. Hence, sensitivity analyses are commonly performed to determine the reactions and species having the largest effects on the resulting model [36]. Improving the quality of those parameters is the priority for the development of an efficient and accurate kinetic mechanism. Some detailed kinetic mechanisms contain some optimized (tuned) parameters. Optimization is a strategy to increase the consistency between model prediction and experimental observation at given conditions. However, there are several problems with tuning:

(1) non-uniqueness: because the model has many parameters, there are many ways to tune them to achieve similar predictions for the limited test data
(2) Sometimes the same data are used for training the parameters and for assessing the performance of the model, i.e., there is no real test set at all.
(3) Sometimes the tweaked values of some parameters assume unphysical values.

To the extent that the tuning takes parameters away from their true physical values, it can make a mechanism less suitable for use as a sub-mechanism that can be reused for other purposes.

We note most procedures used to improve kinetic models depend on the reaction mechanism including all the important reactions, and they can be sensitive to the assumed values of estimated parameters. If the model is missing an important reaction or has inaccurate parameters, the local sensitivity analysis can be misleading. The tuning process is attempting to compensate not just for errors in the initial estimates of the tuned parameters, but also for all the other flaws in the model including any bad values of the un-tuned parameters. Given these variations in the model generation process, different choices potentially result in many different mechanisms. Therefore, the model validation against experimental data is crucial. In the case of oxidation models, it is often performed by comparing numerical predictions against experimental measurements of the laminar burning velocity (S_u), typically at low inlet temperature [37,38], and ignition delay time (IDT), at intermediate or elevated temperatures [39,40]. The experimental values can be affected by the presence of systematic errors due to unstandardized procedures, unknown phenomena, or by differences in the hypotheses adopted for the elaboration of raw

data, resulting in discrepancies between idealized and real conditions. As a way of example, inhomogeneous temperatures and non-zero strain flames produce inconsistent information for IDT and S_u [41], respectively. For this reason, data collected using different setups and methodologies should be considered for robust considerations.
Hence, this work was focused on the development, validation, and evaluation of a theoretically based kinetic mechanism able to reproduce the combustion behavior of light alkenes, which potentially could be used as a reliable sub-mechanism when building mechanisms for other applications (e.g., combustion of heavier fuels). The accuracy of this new mechanism and several previously published mechanisms was evaluated against existing experimental data. The most important reactions were identified via sensitivity analyses to critically discuss various approaches for constructing accurate mechanisms.

2. Methodology

A schematic representation of the methodology adopted in this work for the generation and validation of the detailed kinetic mechanism suitable for light alkene combustion is reported in Figure 1. The workflow is proven to be effective in previous studies [42,43].

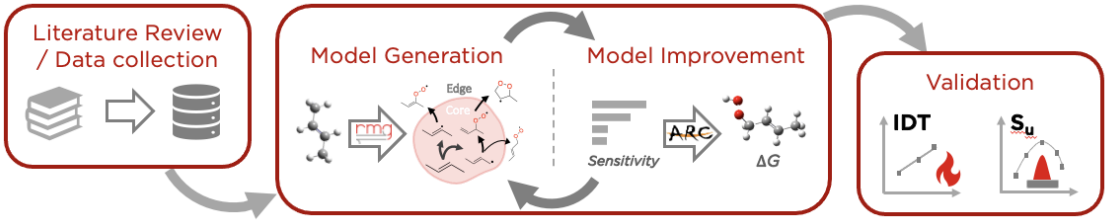

Figure 1. Schematic representation of the procedure adopted in this work for the development and validation of a detailed kinetic mechanism.

2.1 Model Generation

The model generation is facilitated by the automatized tool RMG [33]. As outlined in the introduction section, RMG adopts a rate-based algorithm to automatically select reactions to be included to enlarge the under-generation chemical model iteratively until a user-defined termination criterion is reached. In each iteration, a so-called 'range-based reactor' module is used, where multiple isothermal-isobaric reactors in the transient phase are simulated. The reaction conditions of each simulation are sampled from a range of pre-defined values, namely initial temperature (650 – 1500 K), pressure (0.3 – 100 atm). Within the iterative procedure reported in the previous section, pure fuels in stoichiometric ratio with air were considered at first, to include the most essential pathways and intermediates. The obtained information is gathered in libraries to be used for the sake of model refinement, under the procedure described in the following section. Eventually, an equimolar mixture of ethylene, propylene, and butene isomers in stoichiometric ratio with air was employed for the last iteration. Since combustion processes can cover a large range of temperatures and pressures, using the 'range-based reactor' module helps find the chemistry that is important at different conditions. The model generation at different conditions has allowed for the inclusion of significant pathways relevant for non-stoichiometric compositions too (e.g., pyrolysis), as confirmed by the comparison of estimated against measured S_u and IDT within the range of equivalence ratio 0.3 – 2.0. Additional information on the methodology adopted for the estimation of these parameters as well as data sources will be provided in the following paragraphs. Thermochemical and kinetic data used during the model generation and included in the final model are either taken from appropriate RMG built-in libraries when available or estimated via group additivity (GA) and RMG rate rules, respectively. Many of the sensitive parameters were improved by performing quantum chemistry calculations, as discussed below. In this study, RMG's built-in thermochemistry and kinetic libraries

compiled from the literature [44–48] were used as the starting point. The GA method estimates the missing properties by linear combinations of the corresponding properties of sub-molecular fragments. Rate coefficients are estimated via decision trees trained by RMG built-in training datasets and classified in reaction families based on functional group interactions. Additional information describing RMG software can be found elsewhere [33]. Details on the version of the software and database used and the options and tolerances are given in the Supporting Information.

2.2 Model Improvement

A typical detailed mechanism generated from RMG contains hundreds of species and tens of thousands of reactions, where most of the corresponding parameters are estimated. Sensitivity analyses were performed under several initial conditions relevant to combustion to identify the key parameters with the largest impact on the model predictions. When the accuracy of these parameters is improved, the model is expected to make better predictions of the observables. In the scope of this study, the absolute value of the normalized sensitivity coefficient (*NSC*), as defined in Eq. (1), is calculated:

$$NSC_i = (\mathrm{x}_i^{\mathrm{a}}/y) \cdot \frac{\partial y}{\partial x_i} \quad (1)$$

where x_i represents the generic perturbed variable, namely pre-exponential factor, A, of *i*-th reaction or standard enthalpy of formation, $\Delta H°_{298}$, of *i*-th species, *a* is equal to 1 for pre-exponential factors and null for $\Delta H°_{298}$, and *y* is the generic measurable properties. The mole fraction of ethylene, propylene, butenes, carbon monoxide (CO), hydroxyl radical (OH), formaldehyde (HCHO), formyl radical (HCO), methyl radical (CH_3) are examples of measurables considered in this analysis. By sorting the obtained NSC, the sensitive parameters of our model were found, and if the sensitive parameters are estimates by analogy (e.g., by group additivity) and are not available in the published literature, those parameters were calculated by *ab initio* quantum chemistry methods [49]. The resulting data were added to the thermochemistry library for the following iterations of model generation. This procedure guarantees the identification of the most critical species at any stage, together with an affordable number of quantum mechanics calculations to be performed to build a robust thermochemistry database. More information on our procedure for selecting which species to refine is given in the Supporting Information.

For wells in the potential energy surface (PES), single-point energies, optimized geometries, and harmonic frequencies were calculated using Gaussian 09 [50]. The CBS-QB3 level of theory was utilized, because of its good balance between computational cost and accuracy for hydrocarbon species [51]. If a species contained hindered rotors, rotor scans were performed on the corresponding dihedral angle with 45 steps of 8^o increments (covering 360^o), performing constrained optimizations at each dihedral angle using the B3LYP/CBSB7 level of theory. These DFT energies were used to compute the 1-d hindered rotor potentials. Note B3LYP/CBSB7 is the same level of theory employed for geometry optimizations in the CBS-QB3 calculation procedure. Arkane, a software devoted to statistical mechanical calculations distributed with RMG, was used to calculate thermochemical parameters from the QM outputs, where the rigid rotor harmonic oscillator (RRHO) approximation with 1D separable hindered rotor assumption was utilized. The quantum mechanics calculation workflow is automated by the ARC package, which helps coordinate and troubleshoot the required calculations [49].

2.3 Model Comparison

Different detailed kinetic mechanisms that cover the alkenes of interest and represents the alternative approaches for model generation (e.g., automatically generated or containing tuned parameters) were selected from the literature. The overall reactivity was evaluated by each mechanism and compared with the predictions from the mechanism developed in this work. More specifically, JetSurF [15], LLNL (n-heptane) [17], LLNL (butanol) [18], MIT (butanol)[19], CNRS [25], AramcoMech 3.0 [29], and Creck

[30] models were utilized in this study. The predicted adiabatic isobaric unstrained laminar burning velocities (S_u) and adiabatic isochoric ignition delay times (IDT) of ethylene, propylene, and each butene isomer in the air are computed for each chemistry model using tailor-made tools based on the Cantera package [52]. The S_u simulations were performed by assuming one-dimensional flame, adiabatic and steady-state conditions. The CANTERA software does adaptive meshing to refine the grid used to compute the S_u. This grid refinement is controlled by two user-selected tolerances, "slope", and "curve", respectively representative for threshold values of first and second derivative of the solutions obtained for adjacent cells. Here we used slope=0.07 and curve=0.14. These values were derived from a grid independence analysis [53], and were previously tested for several mechanisms [8]. We tested these tolerances for the new mechanism presented here by cutting the values in half. This only changed Su at 298 K and 1 atm by 0.1%, but significantly increased the CPU time required, so we used slope equal to 0.07 and curve equal to 0.14 in the rest of the calculations. We considered a range of equivalence ratios (φ) defined as:

$$\varphi = \frac{\left({}^{n_f}/_{n_{ox}}\right)}{\left({}^{n_f}/_{n_{ox}}\right)_{st}} \tag{2}$$

where n_f and n_{ox} represent the fuel and oxidizer mole at the actual and the stoichiometric (*st*) conditions, respectively. An initial temperature of 298 K, atmospheric pressure, and φ within the range of 0.4 - 1.8 were considered as initial/boundary conditions for S_u estimations. For the case of mechanisms retrieved from the literature, transport parameters were considered as included in their libraries, whereas the method of estimating transport properties in RMG based on the Joback method was employed for the newly generated mechanism. Regardless of the mechanism considered, a multicomponent transport model neglecting the Soret effect was employed. For the sake of brevity, the assumption of the limited impact of thermal diffusion and Soret effect on the S_u was tested only at stoichiometric conditions, an initial temperature of 298 K, and initial pressure of 1 atm for all the investigated species and models. Results show a deviation lower than 0.002 % concerning the estimation resulting from the simplified assumption, so these phenomena were neglected. The IDTs were computed assuming perfectly premixed air/fuel. Lean, stoichiometric, and rich mixtures with initial temperatures varying from 700 to 1500 K were investigated.

The methods used here to compute $S_u(\varphi)$ and IDT(φ) are widely adopted, and these computed quantities are convenient for comparing fuels. However, we note that the models are idealizations of the experiments, namely perfectly adiabatic and zero flame strain rate were assumed in simulations. Hence, one may also need to be aware of the differences in the posed boundary conditions for thermal and fluid aspects when comparing experimental data with simulation results.

We compare the models with many experiments, so it is convenient to compress the information on the deviations into a few numbers that give an idea of the quality of estimation. Once the generation of the kinetic mechanism was completed, the fractional bias (FB) (Equation 3) and the normalized mean square error (NMSE) (Equation 4) were calculated for the newly generated mechanisms as well as for the ones retrieved in the literature. These parameters compare the generic prediction (*Pr*) obtained at given conditions and the corresponding experimental measurement (*Ex*) to quantify the average difference and overall dispersion, among different datasets. For the sake of simplicity, uncertainties associated with experimental and numerical data were neglected at this stage. This definition of dimensionless parameters uses the same weight for both kinetic indicators (i.e., IDT and S_u) and all experiments.

$$FB = \frac{2\cdot\left[\sum_i^N \alpha_i\cdot(Ex_i - Pr_i)\right]}{\sum_i^N (Ex_i + Pr_i)} \tag{3}$$

$$NMSE = \frac{1}{\mathrm{N}} \cdot \left(\sum_i^N \frac{(Pr_i - Ex_i)^2}{Pr_i \cdot Ex_i} \right) \quad (4)$$

The subscript *i* stands for the i-th observation; *N* represents the number of observations (i.e., the number of experimental data considered in this analysis, collected at the initial conditions reported in Table S1); and α is a coefficient equal to -1 or 1 for S_u and IDT, respectively. α was added to guarantee that if the model consistently overestimates the reactivity, FB will be positive, while if the model consistently underestimates the reactivity FB will be negative. Based on their definition, an ideal model has NMSE and FB equal to zero. Models are considered satisfactory if |FB|< 0.5 and NMSE < 0.3 [54]. Indeed, the former threshold value indicates that the average estimation has an error within ± 40% to the average from the experimental dataset, whereas the latter assess how much the estimations are scattered to experiments.

3. Results and discussion

3.1. Model statistics

The resulting model consists of 797 species and 37 706 reactions. A detailed population analysis for the included species is shown in Figure 2 and Figure 3. Most of the species in the model are radicals. For more information on the radicals see Figure S3 and S4 in the SI. Among these species, 18% of thermochemical data are from the RMG built-in library, while 70% are calculated using CBS-QB3 in this study, covering most of the sensitive thermochemistry. The remaining species are estimated via GA. More insights about the calculated data can be found in Figures S8 - S14.

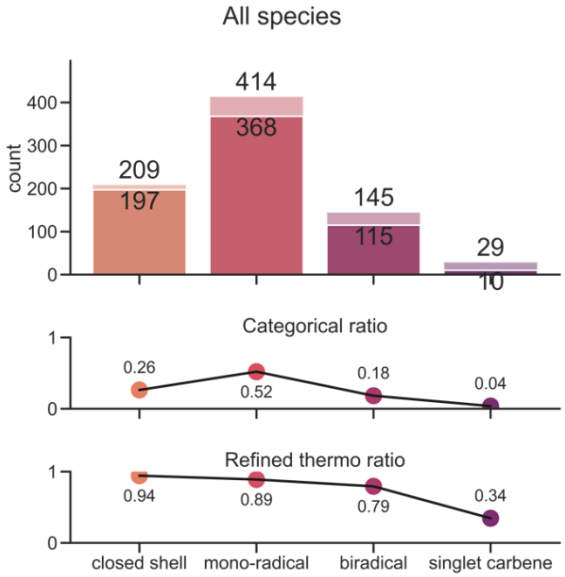

Figure 2. The statistics of species in the model. Species are divided into four categories closed-shell (species without unpaired electrons), mono-radical (species with only one radical site and have an electron multiplicity of 2), biradical, and singlet carbene. The upper bar plot indicates the total number of species and the number with refined thermochemistry parameters in each category. The middle subfigure indicates the population proportion of each category. The bottom subfigure shows the proportion of species with refined thermochemistry in each category.

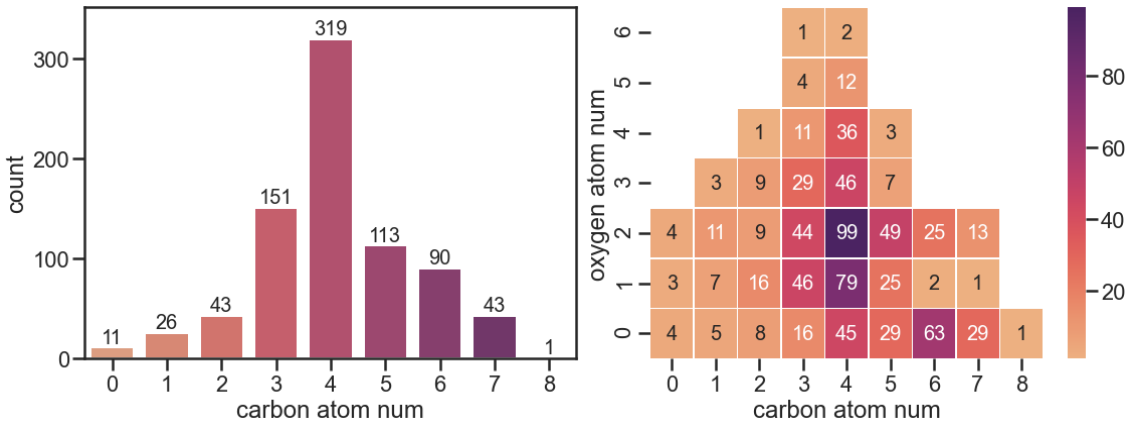

Figure 3. The size distribution of species in the model, by number of carbons (left) and oxygen atoms (right). There are 99 distinct $C_4H_xO_2$ species in the model.

The model includes many C_4 oxygenates, included by RMG as it tries to accurately model the low-temperature (pre-ignition) oxidation chemistry. Species larger than C_4 (including a few benzene derivatives) are also picked by RMG, allowing the model to account for termination reactions and the formation of cyclic species.

3.2. Effectiveness of model refinement

The quality of thermochemical parameters strongly affects the effectiveness of the reaction mechanism generation process and the predictive capability of the resulting mechanism. Thus, iteratively improving the quality of thermochemical parameters is a major strategy to build a better model. The significance of this approach can be understood by comparing the predictions of the mechanisms generated during the iterative procedure. To this aim, statistics on generated mechanisms are briefly summarized (Figure 4, left and Figures S6 and S7), and a comparison of the overall reactivity predicted by these models was performed. For the sake of brevity, only the IDT of 1-butene/air stoichiometric mixture at 10 atm is displayed (Figure 4, right), while other observables showed similar behavior (shown in Figures S1 and S2).

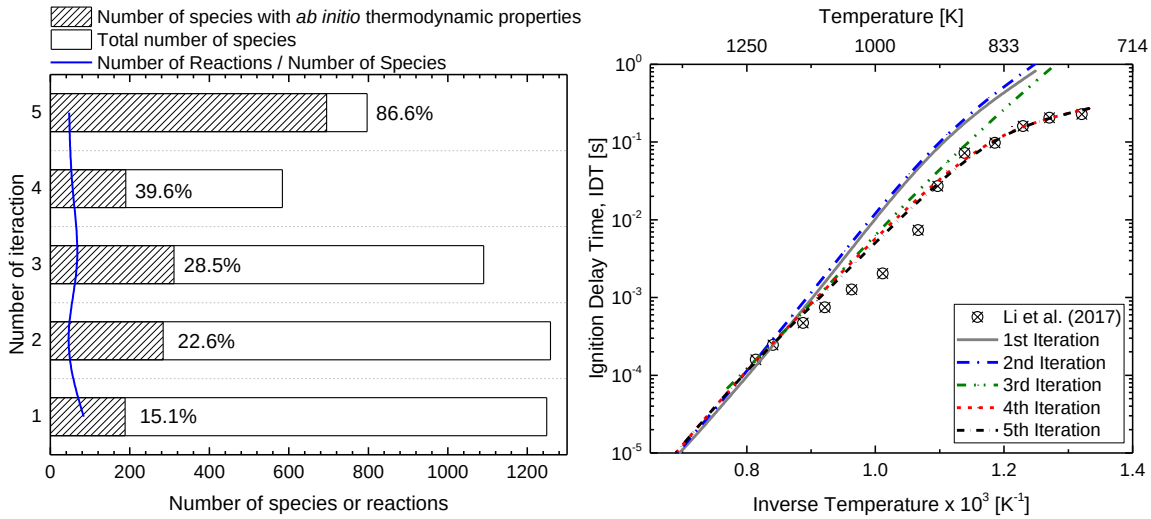

Figure 4. Comparison of the metrics of generated mechanisms (left), estimated and experimental ignition delay time of stoichiometric 1-butene/air mixture at 10 atm as a function of temperature (right). The percentage of the species in the model with ab initio thermochemistry is listed for each iteration. RMG built a model with more than 1000 species at iteration 3. But with higher-accuracy thermochemistry in later iterations RMG decided not all those species are kinetically significant, so the final model is smaller. The later iterations of the model converge to an IDT curve close to the measurements of Li et al. (2017) [55]

Due to the inclusion of a highly reputed C_0-C_2 mechanism from Hashemi et al. [47] as the seed mechanism, high-temperature chemistry is inherently well captured in all of the generated models, so the IDT curves at high-temperature regime are almost invariant across iterations. However, despite the importance of peroxides and their derivatives at low- and intermediate-temperature oxidation, their available accurate data are extraordinary sparse. Hence, particular efforts were put into refining thermochemical parameters of species that are significant at low- and intermediate- temperatures. A large variation in the number of species, reactions and the predicted IDT can be seen when comparing models from the first several iterations. It indicates the incompletion of the refinement, especially for sensitive parameters. For instance, between the second and third iterations, the quantum chemistry calculations corrected the thermochemistry parameters for key intermediates, leading to the inclusion of several important reaction pathways for low- and intermediate- temperature chemistry, causing a faster ignition and a larger model. Further improvements of the thermochemistry for new species generated in the third iteration of the model clarified that some of the pathways included in the third iteration were not competitive, so some species along those pathways are not included in the 4th iteration nor the final model. According to the 4th and 5th iterations, even with a significant increase in the number of species with refined thermochemistry, IDT converges to similar values, indicating the model-construction and refinement process has converged. The distribution of sources for evaluating the species free energies confirms that the generated mechanism does not suffer from bad estimations for sensitive thermo-chemical parameters as can be found in Figure S5. This example shows the effectiveness of improving the quality of thermochemistry data for generating a better kinetic model. We also show that IDT may be used as a monitoring parameter for the status of the iterative procedure adopted for mechanism generation. Under this light, the obtained mechanism is compared below against experimental data and numerical simulations from benchmark models to evaluate its accuracy.

3.3. Model comparison: laminar burning velocity

The S_u is often adopted for the evaluation of the overall reactivity at initial low temperatures and pressures, e.g., 298 K and 1 atm. In this light, experimental values collected by counterflow flame, spherical vessel, and heat flux burner for ethylene [56–60] propylene [3,60–62] and butene isomers [3,25,63–65] in the air were compared with numerical estimations deriving from the abovementioned models. Figure S15 shows the S_u of ethylene and propene, while Figure 5 shows the S_u of butene isomers.

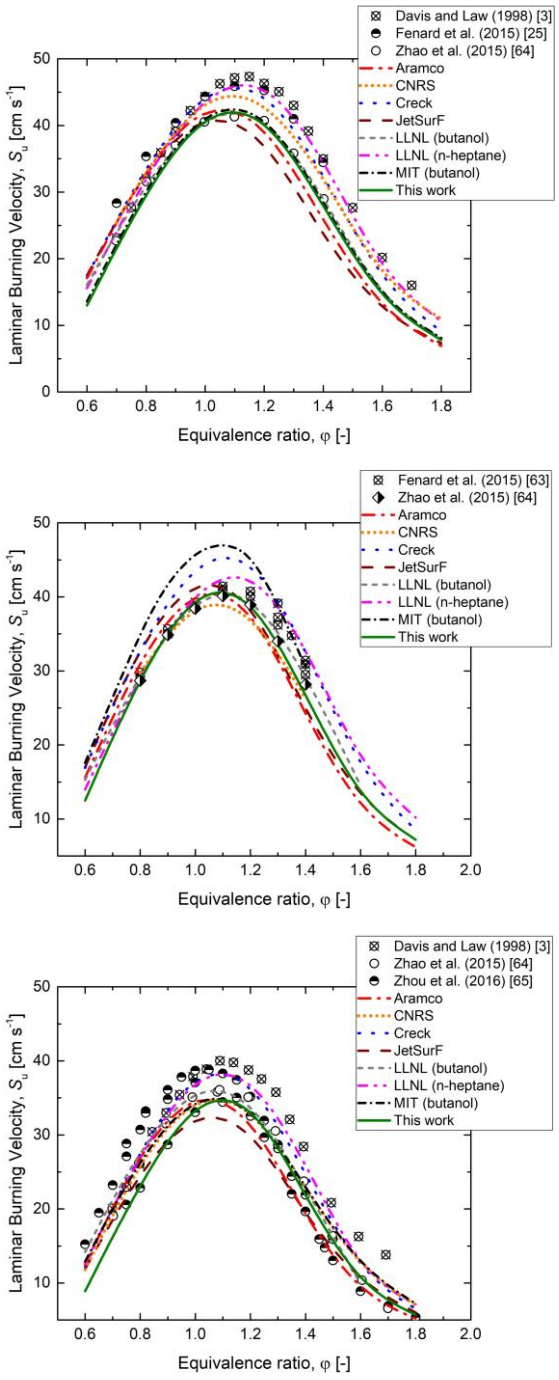

Figure 5. Comparison of experimental measurements (symbols) and numerical estimations (lines) of the laminar burning velocity of 1-C_4H_8 (top), 2-C_4H_8 (middle), and i-C_4H_8 (bottom) vs equivalence ratio at atmospheric conditions. The reference information of mechanisms are highlighted in Table 1.

It is worth mentioning that CNRS, Creck, and LLNL (n-heptane) models tend to generate considerably higher S_u values than the other models, especially for near stoichiometric mixtures. This trend is of particular interest if differences in measured maximum S_u are considered as a function of the year of publication and adopted procedure [66]. This trend can be associated with the evolution of the adopted procedures and experimental systems to measure the S_u. As a way of example, the introduction of non-linear stretch corrections for counterflow flame and spherical vessel methods has strongly decreased the reported S_u of common fuels even at standard conditions [67]. Conversely, flames obtained by flat

burners (e.g., heat flux burner) are implicitly unstretched, thus collected S_u are generally lower than the ones deriving from the other methods [41]. The significance of the effects of the selected apparatus on the S_u can be observed for the case of i-C_4H_8 data reported in Figure 5. Indeed, the measures published by Zhou et al. (2016) [65] show a significant variability at constant initial conditions, especially at lean and near-stoichiometric compositions. These discrepancies are due to the inclusion of measurements deriving from different sources, namely the heat flux burner, constant-volume bomb, and spherical flame method, as reported in the source of data [65].
Regardless of the analyzed fuel, the fundamental laminar burning velocity, i.e., the maximum S_u value can be observed at an equivalence ratio within the range 1.0 – 1.1 for the Aramco and JetSurF models, only. All the other models predict the peak of S_u lies in the interval $1.1 < \varphi < 1.2$. The latter values match typical experimental trends reported for hydrocarbons/air premixed flames under several initial temperatures and pressures [68].

3.4. Model comparison: ignition delay time

To evaluate overall reactivity at intermediate and high temperatures, IDT measurements for ethylene [69], propylene [62], and butene isomers were compared with numerical predictions. Ignition delay times for butene isomers at $\phi = 1$ and $P_0 = 10$ atm were shown in Figure 6, while for the sake of conciseness, data at different conditions (e.g., pressures and equivalence ratios) and data for ethylene and propene are included in the supplementary material (Figures S16 – S20).

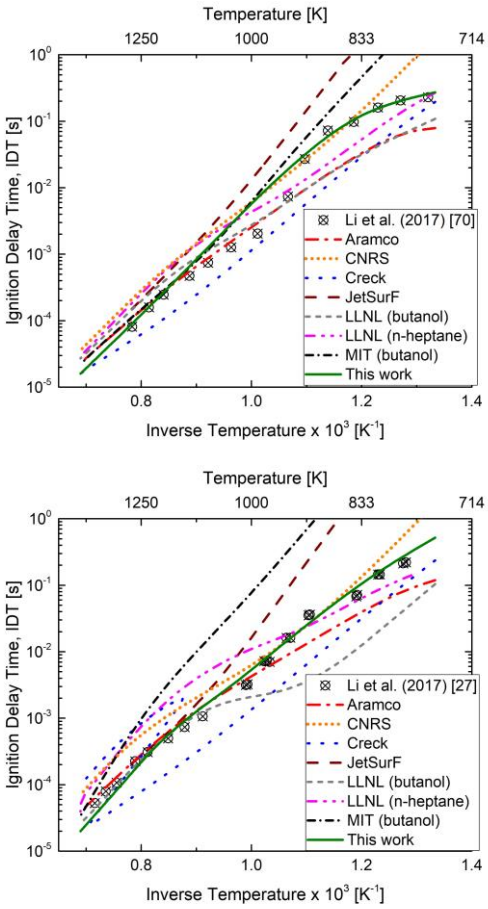

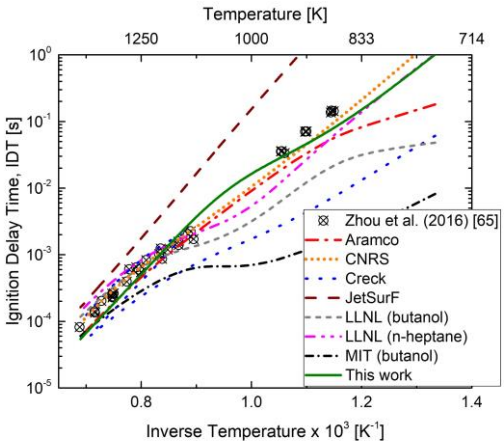

Figure 6. Comparison of experimental measurements (symbols) and numerical estimations (lines) of the ignition delay time IDT of 1-C_4H_8 (top), 2-C_4H_8 (middle), and i-C_4H_8 (bottom) vs temperature in air at stoichiometric composition and 10 atm. The reference information of mechanisms are highlighted in Table 1.

The model produced in this work shows excellent accuracy in IDT data predictions for almost all the investigated conditions. Indeed, only the overall reactivity of 1-butene around 1000 K is slightly underestimated (but still within a factor of 4). Considering the thermal boundary condition adopted in this set of simulations (i.e., adiabatic condition) relevant high-temperature reactions (here coming primarily from [47]) should be also be analyzed. More insights on this topic are discussed below. Besides, it should be noted that Creck and MIT (butanol) indicate i-C_4H_8 as the most reactive butene isomer at a temperature close to 1000 K, in contrast with experimental data and the other mechanisms analyzed in this work. Similar conclusions can be drawn if LLNL (butanol) predictions for 1-C_4H_8 compared with 2-C_4H_8 data at a temperature of ~ 900 K and i-C_4H_8 data at a temperature of ~ 800 K. Aramco shows a satisfactory agreement with the IDT data, except that 1-C_4H_8 reactivity at intermediate temperatures is considerably over predicted. In contrast, large discrepancies between CNRS predictions and experimental data can be observed mainly for ethylene and propylene. This observation can be partially attributed to the limitations in the operating conditions considered in the CNRS model development and validation, namely atmospheric pressure. This suggests that relevant reaction paths ruling ethylene and propylene ignition at higher pressure are missing or inadequately represented in the CNRS model, as supported by the analysis reported in section 3.6 and supplementary materials (chapter 5). The previously reported tendency (for the S_u) of Creck to predict higher reactivity of light alkenes in air, is confirmed for IDT data as well, suggesting the core combustion sub-model in Creck is inaccurate. JetSurF overestimates the reactivity of ethylene and propylene while significantly under-predicting the reactivity of butene isomers (see e.g., Figs S21, S23, S26, S27, and S28). These trends suggest incorrect rates for primary reactions or lack of relevant decomposition pathways, as confirmed by flux diagram analyses reported in the supplementary material (Figures S29 - S33) and sensitivity analyses included in Section 3.6. For all fuels, the LLNL (n-heptane) mechanism provides slightly higher IDT at elevated temperature and lower IDT at intermediate temperature compared to the experimental measurements.

3.5. Model comparison: overall estimation quality

The overall estimation quality resulting from the comparison of different fuels, initial temperatures, pressures, and compositions expressed in terms of absolute values of fractional bias and normalized mean square error (Figure 7) was reported for the investigated models. Different symbols were used to distinguish mechanisms showing negative (-) and positive (+) FBs.

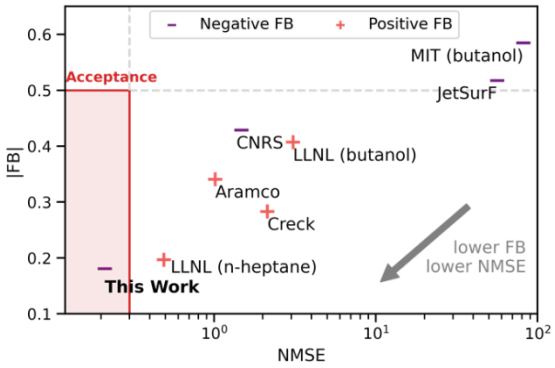

Figure 7. Evaluation of the overall estimation quality for the investigated models, in terms of absolute values of fractional bias (FB) and normalized mean square error (NMSE). Markers are positive and negative signs representing the signs of FBs. The model acceptance criteria are highlighted as the red region based on [53]. The reference information of mechanisms are highlighted in Table 1.

As expected, CNRS, JetSurf, and MIT (butanol) models have significantly negative overall FB, whereas Creck, LLNL (butanol) and LLNL (n-heptane) have positive values, meaning that the first group tends to underpredict the overall reactivity and the second to over predict it. Elevated NMSE values were obtained especially for JetSurf and MIT (butanol). This fact can be mainly attributed to missing important intermediate temperature chemistry, as testified by low accuracy in IDT data reproduction. The overall accuracy of Aramco is strongly affected by 1-C_4H_8 data, where the maximum in FB and NMSE is achieved (see supplementary materials), leading to NMSE equal to 0.64. It is worth noting that all the investigated mechanisms comply with the adopted criterion for FB (i.e., absolute values lower than 0.5) except for JetSurF and MIT (butanol), where FB equal to -0.54 and -0.58 are obtained, respectively. However, only the new model generated in this work respects the NMSE criterion (i.e., NMSE < 0.3), as well. Based on these data it is possible to conclude that our new mechanism represents the most accurate model among the ones analyzed in this work for alkenes combustion. The solid theoretical basis for model development adopted in this work, along with the model's accuracy, favors its use as a building block in mechanisms dedicated to larger compounds. These conditions make it the best candidate for the evaluation of chemical aspects involving alkene oxidation.

3.6. Model comparison: sensitive reactions

To further investigate the causes of the highlighted discrepancies between investigated mechanisms, it is worth identifying the most influential reactions in the system. Besides, this analysis also provides a foundational understanding of further improving the alkene model in the future.

At the investigated conditions, the chemistry of HO_2 and radical addition has been confirmed as impacting factors, as shown by the sensitivity analyses at different compositions and T of 700 K and P of 10 atm, for the butene isomers (Figure 8). The homologous data for ethylene and propylene are reported in Figures S21 and S24. According to the sensitivity analysis, HO_2 addition reactions have one of the largest positive impacts on OH radical generation, therefore strongly promoting the general reactivity. However, rate coefficients of those reactions in analyzed mechanisms show significant discrepancies, and it is worth noting that rate coefficients included in the current model are derived from quantum mechanical calculations (at the CBS-QB3 level of theory recorded in the RMG database). Given the importance of butene + HO_2 reactions identified by our model, some inconsistencies in the inclusion of these reactions and their rate coefficients can be observed. In particular, 1-C_4H_8 + HO_2 ⇋ CC[CH]COO is exclusively included in LLNL (heptane), Aramco, LLNL (butanol), and the newly generated mechanism. 2-C_4H_8 +HO_2 ⇋ C[CH]C(C)OO is missing in JetSurf, CNRS, MIT (butanol), and Creck, and rate coefficients from models containing the reaction are within one order of magnitude,

regardless of the adopted sources (parameters in Aramco and LLNL (butanol) are calculated at QCISD(T)/cc-pV∞Z//B3LYP/6-311++G(d,p) by Zador et al. (2011) [71], whereas the mechanism generated in this work has coefficients calculated at CBS-QB3 level of theory). JetSurf, CNRS, and MIT (butanol) do not include the reaction i-C_4H_8 + HO_2 ⇋ C[C](C)COO, while Creck uses a considerably larger rate coefficient than any of the other mechanisms including this reaction (i.e., LLNL (heptane), Aramco, LLNL (butanol), and newly generated mechanism).

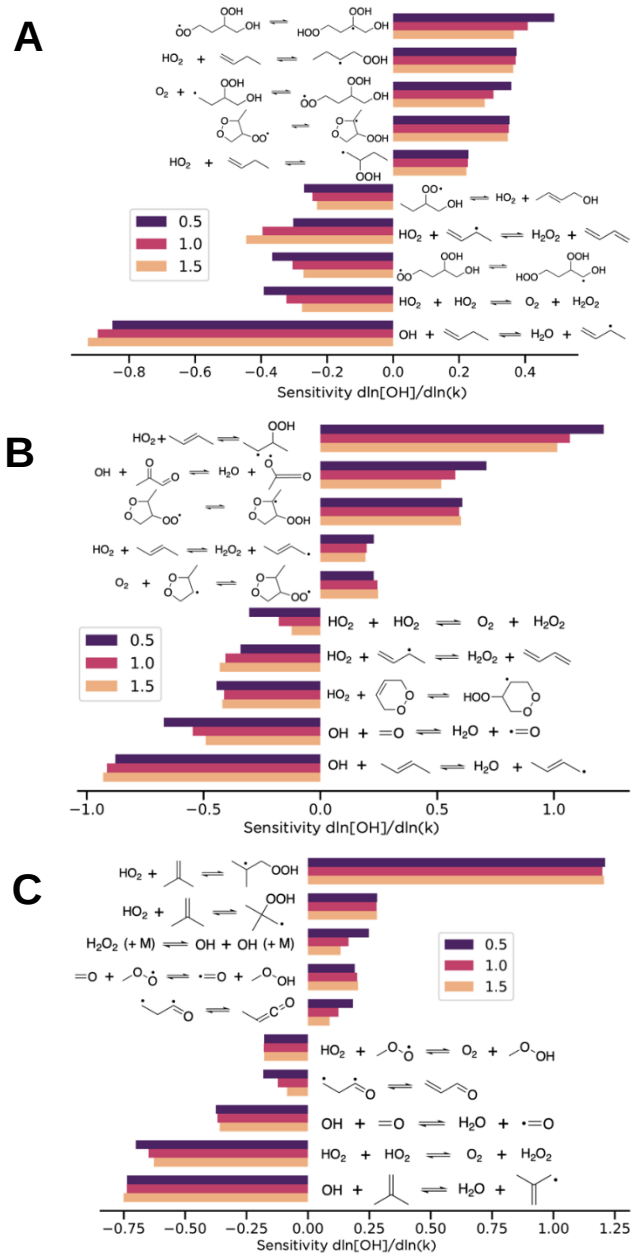

Figure 8. Sensitivity analysis of OH radical concentration at 10% fuel depletion at T = 700 K, P = 10 atm, φ = 0.5, 1.0, and 1.5. The fuels shown are 1-butene (A), 2-butene (B), and iso-butene (C).

Regardless of the analyzed fuel, sensitivity analyses also indicate that hydrogen abstraction by small radicals plays a significant role in primary radical production, especially at low and intermediated temperatures [72]. For the sake of clarity, Figure 8 reported a shortlist of reactions with large NSC.

However, considering a larger group of reactions, a reduced list of hydrogen abstraction reactions having a significant impact on the resulting model can be drawn. Besides, relevant reactions for C_2 chemistry, as highlighted by Xu and Konnov [73], were also considered in this stage to compare the core mechanisms included in the analyzed models. The sensitive reactions are reported in Table S2 together with the sources utilized by the different models for the determination of the corresponding rate coefficients.

The rate coefficients used in various models for a few of the most important reactions are shown in Figure 9. A more comprehensive dataset is reported in the supplementary information, including reactions consuming C_2H_4 (Fig S22) and C_2H_3 (Fig S23). C_3 and C_4 chemistry are compared in terms of hydrogen abstraction by OH and H (Figs S25 - S28).

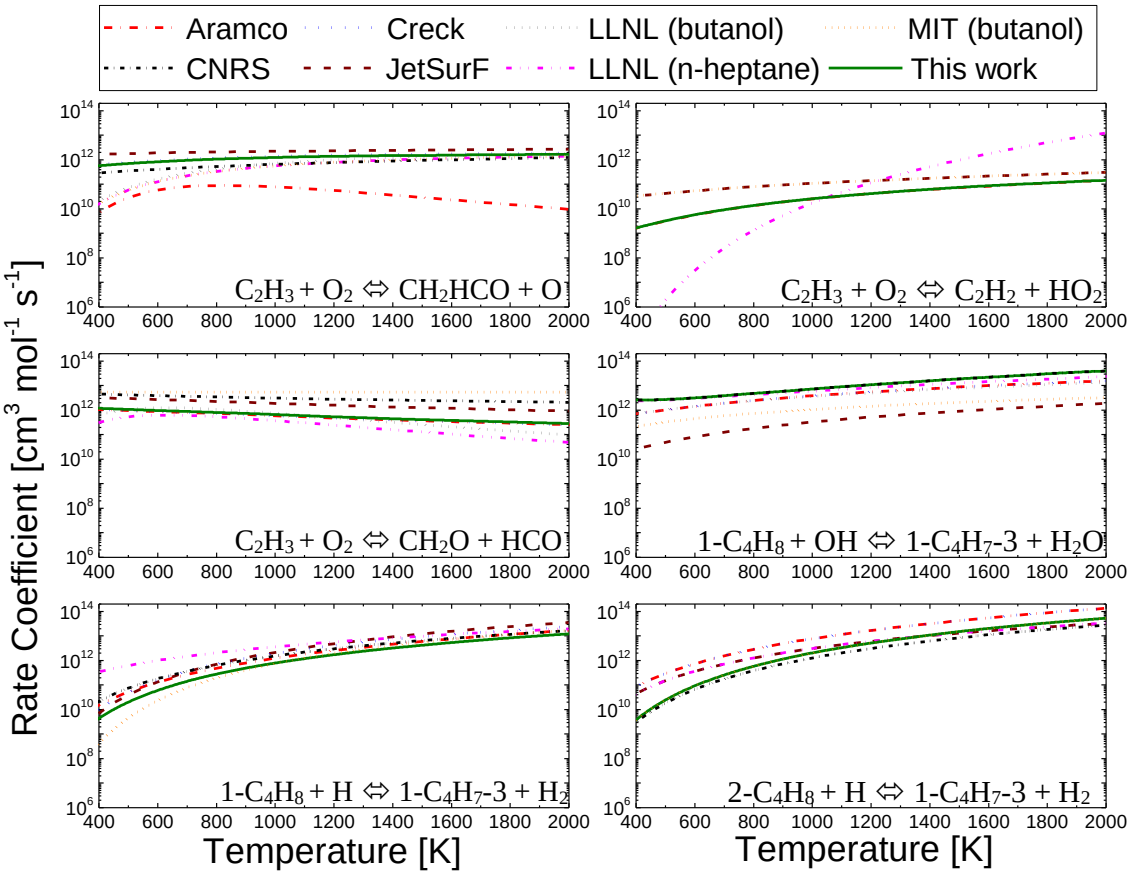

Figure 9. Comparison of some influential reaction rates at 10 bar for light alkene combustion as included in the analyzed mechanisms. The reference information of mechanisms are highlighted in Table 1.

Although different sources are employed for the case of hydrogen abstraction by OH from C_2H_4 and hydrogen abstraction by OH and H from C_3H_6, similar rates can be observed for all the analyzed mechanisms, demonstrating the robustness of the data utilized. On the other hand, Creck and JetSurF include considerably higher rate coefficients for hydrogen abstraction by OH from C_2H_4 and H from C_3H_6, especially at temperatures lower than 1200 K. This discrepancy may be a possible source of inaccuracy in the estimation of IDT, reported for ethylene containing mixture. It should be emphasized that LLNL (n-heptane) includes estimated coefficients for $C_2H_3 + O_2 \Leftrightarrow C_2H_2 + HO_2$ providing higher values at high temperatures and lower values at low- and intermediate-temperatures than the rates from QM calculations [47,74]. Meanwhile, its rate coefficients for $C_2H_3 + O_2 \Leftrightarrow CH_2O + HCO$ are the lowest for all the investigated temperatures. They hinder the production of reactive species at elevated temperatures and lead to discrepancies in branching ratios and ignition behavior, potentially explaining

the general observation reported for IDT values. Conversely, kinetics for $C_2H_2 + HO_2$ and $CH_2O + HCO$ production in MIT (butanol) mechanism have weak temperature dependencies. Moreover, the latter has the largest values for all the investigated temperatures, in contrast with the indications suggested by the majority of the mechanisms and quantum mechanical calculations published by Goldsmith et al. (2015) [74], where the rate of $CH_2O + HCO$ decreases and CH_2CHO formation is favored with increasing temperatures. It is also worth mentioning that most of the calculated coefficients included in the analyzed mechanisms for the reactions involving $C_2H_3 + O_2$ are pressure-dependent (Please refer to Table S2 for further information). It rationalizes the absence of this reaction in the model generated at atmospheric pressure, i.e., CNRS. Hence, the lack of a proper description of the C_2H_3 chemistry in the CNRS model can explain its poor predictive quality in ethylene and propylene IDT.

Regarding C_4 chemistry, large differences can be observed between the analyzed mechanisms. In particular, the rate coefficients for H abstractions by OH from 1-C_4H_8 and 2-C_4H_8 included in JetSurF and MIT (butanol) are up to two orders of magnitude smaller than literature rates [75–77]. Besides, estimated coefficients reported in LLNL (n-heptane) for 1-C_4H_8 lead to faster hydrogen abstraction by H radical at temperature < 1000 K, possibly causing the too-fast ignition of the LLNL (n-heptane) model at those conditions.

4. Conclusions

The main goal of this study was the development and validation of a detailed kinetic mechanism suitable for the estimation of light alkenes combustion up to butene isomers in a wide range of conditions. It was analyzed and compared with models and experiments retrieved in the literature. The mechanism produced in this work was found the most accurate for the estimation of the laminar burning velocity and ignition delay time of light alkenes. The absence of tuned parameters makes this model appropriate as a possible core model. Thermochemical parameters for more than 550 species were refined via *ab initio* calculations, significantly improving the accuracy of the model predictions e.g., of IDTs. Rate coefficients of several relevant reactions, including HO_2 addition and hydrogen abstraction by OH and H of investigated fuels, were compared. Possible explanations for some of the discrepancies observed between models from the literature were identified and discussed. We hope the identification here of many sensitive reactions and literature discrepancies on rate coefficients will inspire work to measure or calculate more accurate rate coefficients for these reactions, to complement the improved thermochemical parameters reported here. The new mechanism was used to clarify the reaction paths important in the pre-ignition and combustion chemistry of light alkenes, laying the foundations for a comprehensive combustion core model.

Acknowledgement
This work was conducted as part of the Co-Optimization of Fuels & Engines (Co-Optima) project sponsored by the U.S. Department of Energy (DOE) Office of Energy Efficiency and Renewable Energy (EERE) [grant number DE-EE0007982].

Supplementary material
Supplementary material associated with this article includes the newly generated mechanism in various formats, data visualization of the model statistics, complementary flux diagram and comparison of analyzed mechanisms in terms of laminar burning velocity, ignition delay time, and rate coefficients of sensitive reactions.

References

[1] T. Lu, C.K. Law, Toward accommodating realistic fuel chemistry in large-scale computations, Progress in Energy and Combustion Science. 35 (2009) 192–215.

[2] G. Pio, E. Salzano, Implementation of Gas-Phase Kinetic Model for the Optimization of the Ethylene Oxide Production, Chemical Engineering Science. 212 (2020) 115331.

[3] S.G. Davis, C.K. Law, Determination of and Fuel Structure Effects on Laminar Flame Speeds of C1 to C8 Hydrocarbons, Combustion Science and Technology. 140 (1998) 427–449.

[4] Y. Zhang, J. Cai, L. Zhao, J. Yang, H. Jin, Z. Cheng, Y. Li, L. Zhang, F. Qi, An experimental and kinetic modeling study of three butene isomers pyrolysis at low pressure, Combustion and Flame. 159 (2012) 905–917.

[5] F. Battin-Leclerc, Detailed chemical kinetic models for the low-temperature combustion of hydrocarbons with application to gasoline and diesel fuel surrogates, Progress in Energy and Combustion Science. 34 (2008) 440–498.

[6] F. Battin-Leclerc, Development of kinetic models for the formation and degradation of unsaturated hydrocarbons at high temperature, Physical Chemistry Chemical Physics. 4 (2002) 2072–2078.

[7] A. Jach, W. Rudy, A. Pękalski, A. Teodorczyk, Assessment of detailed reaction mechanisms for reproduction of ignition delay times of C2–C6 alkenes and acetylene, Combustion and Flame. 206 (2019) 37–50.

[8] G. Pio, V. Palma, E. Salzano, Comparison and validation of detailed kinetic models for the oxidation of light alkenes, Ind. Eng. Chem. Res. 57 (2018) 7130–7135.

[9] S.G. Davis, C.K. Law, H. Wang, Propene pyrolysis and oxidation kinetics in a flow reactor and laminar flames, Combustion and Flame. 119 (1999) 375–399.

[10] W. Gardiner, V. Lissianski, Z. Qin, G. Smith, D. Golden, M. Frenklach, B. Eiteneer, M. Goldenberg, N. Moriarty, C. Bowman, R. Hanson, S. Song, C. Schmidt, R. Serauskas, The GRI-Mech(TM) Model for Natural Gas Combustion and NO Formation and Removal Chemistry, in: Fifth International Conference on Technologies and Combustion for a Clean Environment, 1999.

[11] A.A. Konnov, Development and validation of a detailed reaction mechanism for the combustion of small hydrocarbons, in: International Symposium on Combustion, Edinburgh, UK, 2000: p. 317.

[12] A. Frassoldati, T. Faravelli, E. Ranzi, Kinetic modeling of the interactions between NO and hydrocarbons at high temperature, Combustion and Flame. 135 (2003) 97–112.

[13] G. Blanquart, H. Pitsch, Thermochemical properties of Polycyclic Aromatic Hydrocarbons (PAH) from G3MP2B3 calculations, Journal of Physical Chemistry A. 111 (2007) 6510–6520.

[14] H. Wang, USC Mech Version II, Journal of Chemical Information and Modeling. 53 (2013) 1689–1699.

[15] H. Wang, E. Dames, B. Sirjean, D.A. Sheen, R. Tango, A. Violi, J.Y.W. Lai, F.N. Egolfopoulos, D.F. Davidson, R.K. Hanson, C.T. Bowman, C.K. Law, W. Tsang, N.P. Cernansky, D.L. Miller, R.P. Lindstedt, A high-temperature chemical kinetic model of n-alkane (up to n-dodecane), cyclohexane, and methyl-, ethyl-, n-propyl and n-butyl-cyclohexane oxidation at high temperatures, JetSurF version 2.0, September 19, 2010 (http://web.stanford.edu/group/haiwanglab/, (n.d.).

[16] D. Healy, D.M. Kalitan, C.J. Aul, E.L. Petersen, G. Bourque, H.J. Curran, Oxidation of C1-C5 alkane quinternary natural gas mixtures at high pressures, Energy and Fuels. 24 (2010) 1521–1528.

[17] M. Mehl, W.J. Pitz, C.K. Westbrook, H.J. Curran, Kinetic modeling of gasoline surrogate components and mixtures under engine conditions, Proceedings of the Combustion Institute. 33 (2011) 193–200.

[18] S.M. Sarathy, S. Vranckx, K. Yasunaga, M. Mehl, P. Oswald, W.K. Metcalfe, C.K. Westbrook, W.J. Pitz, K. Kohse-Hoinghaus, R.X. Fernandes, H.J. Curran, A comprehensive chemical kinetic combustion model for the four butanol isomers, Combustion and Flame. 159 (2012) 2028–2055.

[19] M.R. Harper, K.M. Van Geem, S.P. Pyl, G.B. Marin, W.H. Green, Comprehensive reaction mechanism for n-butanol pyrolysis and combustion, Combustion and Flame. 158 (2011) 16–41.

[20] M. Schenk, L. Leon, K. Moshammer, P. Oßwald, T. Zeuch, L. Seidel, F. Mauss, K. Kohse-Höinghaus, Detailed mass spectrometric and modeling study of isomeric butene flames, Combustion and Flame. 160 (2013) 487–503.

[21] E. Ranzi, A. Frassoldati, R. Grana, A. Cuoci, T. Faravelli, A.P. Kelley, C.K. Law, Hierarchical and comparative kinetic modeling of laminar flame speeds of hydrocarbon and oxygenated fuels, Progress in Energy and Combustion Science. 38 (2012) 468–501.

[22] University of California at San Diego, Chemical-Kinetic Mechanisms for Combustion Applications, (n.d.).

[23] J. Bugler, K.P. Somers, E.J. Silke, H.J. Curran, Revisiting the Kinetics and Thermodynamics of the Low-Temperature Oxidation Pathways of Alkanes: A Case Study of the Three Pentane Isomers, Journal of Physical Chemistry A. 119 (2015) 7510–7527.

[24] K. Zhang, C. Banyon, C. Togbé, P. Dagaut, J. Bugler, H.J. Curran, An experimental and kinetic modeling study of n-hexane oxidation, Combustion and Flame. 162 (2015) 4194–4207.

[25] Y. Fenard, G. Dayma, F. Halter, F. Foucher, Z. Serinyel, P. Dagaut, Experimental and modeling study of the oxidation of 1-butene and cis -2-butene in a jet-stirred reactor and a combustion vessel, Energy and Fuels. 29 (2015) 1107–1118.

[26] K. Zhang, C. Banyon, J. Bugler, H.J. Curran, A. Rodriguez, O. Herbinet, F. Battin-Leclerc, C. B'Chir, K.A. Heufer, An updated experimental and kinetic modeling study of n-heptane oxidation, Combustion and Flame. 172 (2016) 116–135.

[27] Y. Li, C.W. Zhou, K.P. Somers, K. Zhang, H.J. Curran, The oxidation of 2-butene: A high pressure ignition delay, kinetic modeling study and reactivity comparison with isobutene and 1-butene, Proceedings of the Combustion Institute. 36 (2017) 403–411.

[28] G. Capriolo, V.A. Alekseev, A.A. Konnov, An experimental and kinetic study of propanal oxidation, Combustion and Flame. 197 (2018) 11–21.

[29] C.W. Zhou, Y. Li, U. Burke, C. Banyon, K.P. Somers, S. Ding, S. Khan, J.W. Hargis, T. Sikes, O. Mathieu, E.L. Petersen, M. AlAbbad, A. Farooq, Y. Pan, Y. Zhang, Z. Huang, J. Lopez, Z. Loparo, S.S. Vasu, H.J. Curran, An experimental and chemical

kinetic modeling study of 1,3-butadiene combustion: Ignition delay time and laminar flame speed measurements, Combustion and Flame. 197 (2018) 423–438.
[30] W. Pejpichestakul, E. Ranzi, M. Pelucchi, A. Frassoldati, A. Cuoci, A. Parente, T. Faravelli, Examination of a soot model in premixed laminar flames at fuel-rich conditions, Proceedings of the Combustion Institute. 37 (2019) 1013–1021.
[31] W. Li, G. Wang, Y. Li, T. Li, Y. Zhang, C. Cao, J. Zou, C.K. Law, Experimental and kinetic modeling investigation on pyrolysis and combustion of n-butane and i-butane at various pressures, Combustion and Flame. 191 (2018) 126–141.
[32] N.M. Vandewiele, K.M. Van Geem, M.F. Reyniers, G.B. Marin, Genesys: Kinetic model construction using chemo-informatics, Chemical Engineering Journal. 207–208 (2012) 526–538.
[33] C.W. Gao, J.W. Allen, W.H. Green, R.H. West, Reaction Mechanism Generator: Automatic construction of chemical kinetic mechanisms, Computer Physics Communications. 203 (2016) 212–225.
[34] H.J. Curran, Developing detailed chemical kinetic mechanisms for fuel combustion, Proceedings of the Combustion Institute. 37 (2019) 57–81.
[35] S.W. Benson, Thermochemical Kinetics: Methods for the Estimation of Thermochemical Data and Rate Parameters, in: Thermochemical Kinetics., 2nd ed., John Wiley & Sons, Inc., Hoboken, USA, 1976.
[36] A. Varma, M. Morbidelli, H. Wu, Parametric sensitivity in chemical systems, 1st ed., Cambridge University Press, Cambridge, UK, 1999.
[37] F.N. Egolfopoulos, N. Hansen, Y. Ju, K. Kohse-Hoinghaus, C.K. Law, F. Qi, Advances and challenges in laminar flame experiments and implications for combustion chemistry, Progress in Energy and Combustion Science. 43 (2014) 36–67.
[38] G. Pio, E. Salzano, Laminar Burning Velocity of Methane, Hydrogen, and Their Mixtures at Extremely Low-Temperature Conditions, Energy & Fuels. 32 (2018) 8830–8836.
[39] J.M. Simmie, Detailed chemical kinetic models for the combustion of hydrocarbon fuels, Progress in Energy and Combustion Science. 29 (2003) 599–634.
[40] H. Wang, D.A. Sheen, Combustion kinetic model uncertainty quantification, propagation and minimization, Progress in Energy and Combustion Science. 47 (2015) 1–31.
[41] V.A. Alekseev, A.A. Konnov, Data consistency of the burning velocity measurements using the heat flux method: Hydrogen flames, Combustion and Flame. 194 (2018) 28–36.
[42] X. Dong, E. Ninnemann, D.S. Ranasinghe, A. Laich, R. Greene, S.S. Vasu, W.H. Green, Revealing the critical role of radical-involved pathways in high temperature cyclopentanone pyrolysis, Combustion and Flame. 216 (2020) 280–292.
[43] R.J. Gillis, W.H. Green, Thermochemistry Prediction and Automatic Reaction Mechanism Generation for Oxygenated Sulfur Systems: A Case Study of Dimethyl Sulfide Oxidation, ChemSystemsChem. (2020).
[44] A. Burcat, R. Branko, Third millennium ideal gas and condensed phase thermochemical database for combustion with updates from active thermochemical tables, Technical Report. ANL-05/20 (2005) ANL-05/20 TAE 960.
[45] C.L. Yaws, Yaws' Critical Property Data for Chemical Engineers and Chemists, Http://App.Knovel.Com/Hotlink/Toc/Id:KpYCPDCECD/Yaws-Critical-Property/Yaws-Critical-Property. (2014).
[46] M.P. Burke, S.J. Klippenstein, L.B. Harding, A quantitative explanation for the apparent anomalous temperature dependence of OH + HO2=H2O+O2 through multi-scale modeling, Proceedings of the Combustion Institute. 34 (2013) 547–555.
[47] H. Hashemi, J.M. Christensen, S. Gersen, H. Levinsky, S.J. Klippenstein, P. Glarborg, High-pressure oxidation of methane, Combustion and Flame. 172 (2016) 349–364.
[48] X. Li, A.W. Jasper, J. Zádor, J.A. Miller, S.J. Klippenstein, Theoretical kinetics of O + C2H4, Proceedings of the Combustion Institute. 36 (2017) 219–227.
[49] A. Grinberg Dana, D. Ranasinghe, H. Wu, C. Grambow, X. Dong, M. Johnson, M. Goldman, M. Liu, W.H. Green, "ARC - Automated Rate Calculator", version 1.1.0, DOI: 10.5281/Zenodo.3356849. (n.d.) https://github.com/ReactionMechanismGenerator/ARC.
[50] M.J. Frisch, G.W. Trucks, H.B. Schlegel, G.E. Scuseria, M.A. Robb, J.R. Cheeseman, G. Scalmani, V. Barone, B. Mennucci, G.A. Petersson, H. Nakatsuji, M. Caricato, X. Li, H.P. Hratchian, A.F. Izmaylov, J. Bloino, G. Zheng, J.L. Sonnenberg, M. Hada, M. Ehara, K. Toyota, R. Fukuda, J. Hasegawa, M. Ishida, T. Nakajima, Y. Honda, O. Kitao, H. Nakai, T. Vreven, J.A. Montgomery, J.E. Peralta, F. Ogliaro, M. Bearpark, J.J. Heyd, E. Brothers, K.N. Kudin, V.N. Staroverov, R. Kobayashi, J. Normand, K. Raghavachari, A. Rendell, J.C. Burant, S.S. Iyengar, J. Tomasi, M. Cossi, N. Rega, J.M. Millam, M. Klene, J.E. Knox, J.B. Cross, V. Bakken, C. Adamo, J. Jaramillo, R. Gomperts, R.E. Stratmann, O. Yazyev, A.J. Austin, R. Cammi, C. Pomelli, J.W. Ochterski, R.L. Martin, K. Morokuma, V.G. Zakrzewski, G.A. Voth, P. Salvador, J.J. Dannenberg, S. Dapprich, A.D. Daniels, Farkas, J.B. Foresman, J. V Ortiz, J. Cioslowski, D.J. Fox, Gaussian 09, Gaussian 09, Revision B.01, Gaussian, Inc., Wallingford CT. (2009).
[51] F.C. Pickard, E.K. Pokon, M.D. Liptak, G.C. Shields, Comparison of CBS-QB3, CBS-APNO, G2, and G3 thermochemical predictions with experiment for formation of ionic clusters of hydronium and hydroxide ions complexed with water, Journal of Chemical Physics. 122 (2005) 1–7.
[52] D.G. Goodwin, An Open Source, Extensible Software Suite FOR CVD Process Simulation, 2003.
[53] G. Pio, E. Salzano, The effect of ultra-low temperature on the flammability limits of a methane/air/diluent mixtures, Journal of Hazardous Materials. 362 (2019) 224–229.
[54] V.C. Patel, A. Kumar, Evaluation of three air dispersion models: ISCST2, ISCLT2, and SCREEN2 for mercury emissions in an urban area, Environmental Monitoring and Assessment. 53 (1998) 259–277.
[55] Y. Li, E.O. Connor, C. Zhou, H.J. Curran, An Experimental Study of Butene Isomers and 1 , 3-Butadiene Ignition Delay Times at Elevated Pressures, (2016) 1–6.
[56] F.N. Egolfopoulos, D.L. Zhu, C.K. Law, Experimental and numerical determination of laminar flame speeds: Mixtures of C2-hydrocarbons with oxygen and nitrogen, Symposium (International) on Combustion. 23 (1991) 471–478.

[57] M.I. Hassan, K.T. Aung, O.C. Kwon, G.M. Faeth, Properties of Laminar Premixed Hydrocarbon/Air Flames at Various Pressures, JOURNAL OF PROPULSION AND POWER. 14 (1998) 479–492.
[58] T. Hirasawa, C.J. Sung, A. Joshi, Z. Yang, H. Wang, C.K. Law, Determination of laminar flame speeds using digital particle image velocimetry: Binary Fuel blends of ethylene, n-Butane, and toluene, Proceedings of the Combustion Institute. 29 (2002) 1427–1434.
[59] K. Kumar, G. Mittal, C.J. Sung, C.K. Law, An experimental investigation of ethylene/O2/diluent mixtures: Laminar flame speeds with preheat and ignition delays at high pressures, Combustion and Flame. 153 (2008) 343–354.
[60] G. Pio, A. Ricca, V. Palma, E. Salzano, Low temperature combustion of methane/alkenes mixtures, Fuel. 254 (2019) 115567.
[61] G. Jomaas, X.L. Zheng, D.L. Zhu, C.K. Law, Experimental determination of counterflow ignition temperatures and laminar flame speeds of C2-C3hydrocarbons at atmospheric and elevated pressures, Proceedings of the Combustion Institute. 30 (2005) 193–200.
[62] S.M. Burke, U. Burke, R. Mc Donagh, O. Mathieu, I. Osorio, C. Keesee, A. Morones, E.L. Petersen, W. Wang, T.A. DeVerter, M.A. Oehlschlaeger, B. Rhodes, R.K. Hanson, D.F. Davidson, B.W. Weber, C.J. Sung, J. Santner, Y. Ju, F.M. Haas, F.L. Dryer, E.N. Volkov, E.J.K. Nilsson, A.A. Konnov, M. Alrefae, F. Khaled, A. Farooq, P. Dirrenberger, P.A. Glaude, F. Battin-Leclerc, H.J. Curran, An experimental and modeling study of propene oxidation. Part 2: Ignition delay time and flame speed measurements, Combustion and Flame. 162 (2015) 296–314.
[63] Y. Fenard, P. Dagaut, G. Dayma, F. Halter, F. Foucher, Experimental and kinetic modeling study of trans-2-butene oxidation in a jet-stirred reactor and a combustion bomb, Proceedings of the Combustion Institute. 35 (2015) 317–324.
[64] P. Zhao, W. Yuan, H. Sun, Y. Li, A.P. Kelley, X. Zheng, C.K. Law, Laminar flame speeds, counterflow ignition, and kinetic modeling of the butene isomers, Proceedings of the Combustion Institute. 35 (2015) 309–316.
[65] C.W. Zhou, Y. Li, E. O'Connor, K.P. Somers, S. Thion, C. Keesee, O. Mathieu, E.L. Petersen, T.A. DeVerter, M.A. Oehlschlaeger, G. Kukkadapu, C.J. Sung, M. Alrefae, F. Khaled, A. Farooq, P. Dirrenberger, P.A. Glaude, F. Battin-Leclerc, J. Santner, Y. Ju, T. Held, F.M. Haas, F.L. Dryer, H.J. Curran, A comprehensive experimental and modeling study of isobutene oxidation, Combustion and Flame. 167 (2016) 353–379.
[66] C.K. Law, Fuel options for next-generation chemical propulsion, AIAA Journal. 50 (2012) 19–36.
[67] V.A. Alekseev, M. Christensen, E. Berrocal, E.J.K. Nilsson, A.A. Konnov, Laminar premixed flat non-stretched lean flames of hydrogen in air, Combustion and Flame. 162 (2015) 4063–4074.
[68] A.A. Konnov, A. Mohammad, V.R. Kishore, N. Il Kim, C. Prathap, S. Kumar, A comprehensive review of measurements and data analysis of laminar burning velocities for various fuel+air mixtures, Progress in Energy and Combustion Science. 68 (2018) 197–267.
[69] O.G. Penyazkov, K.L. Sevrouk, V. Tangirala, N. Joshi, High-pressure ethylene oxidation behind reflected shock waves, Proceedings of the Combustion Institute. 32 II (2009) 2421–2428.
[70] Y. Li, C.W. Zhou, H.J. Curran, An extensive experimental and modeling study of 1-butene oxidation, Combustion and Flame. 181 (2017) 198–213.
[71] J. Zádor, S.J. Klippenstein, J.A. Miller, Pressure-dependent OH yields in alkene + HO2 reactions: A theoretical study, Journal of Physical Chemistry A. 115 (2011) 10218–10225.
[72] I. Glassman, R.A. Yetter, Combustion, 4th ed., Elsevier, San Diego, California, 2008.
[73] C. Xu, A.A. Konnov, Validation and analysis of detailed kinetic models for ethylene combustion, Energy. 43 (2012) 19–29.
[74] C.F. Goldsmith, L.B. Harding, Y. Georgievskii, J.A. Miller, S.J. Klippenstein, Temperature and pressure dependent rate coefficients for the reaction of vinyl radical with molecular oxygen, The Journal of Physical Chemistry A. 119 (2015) 7766–7779.
[75] W. Tsang, Chemical Kinetic Data Base for Combustion Chemistry Part V. Propene, Journal of Physical and Chemical Reference Data. 20 (1991) 221.
[76] H. Sun, C.K. Law, Kinetics of hydrogen abstraction reactions of butene isomers by OH radical, Journal of Physical Chemistry A. 114 (2010) 12088–12098.
[77] K.M. Van Geem, S.P. Pyl, G.B. Marin, M.R. Harper, W.H. Green, Accurate high-temperature reaction networks for alternative fuels: Butanol isomers, Industrial and Engineering Chemistry Research. 49 (2010) 10399–10420.